Available online at www.sciencedirect.com
ScienceDirect
Journal of Sound and Vibration 299 (2007) 720–738
JOURNAL OF SOUND AND VIBRATION
www.elsevier.com/locate/jsvi

Exact vibration analysis of variable thickness thick annular isotropic and FGM plates

E. Efraim, M. Eisenberger*

Faculty of Civil and Environmental Engineering, Technion-Israel Institute of Technology, Technion City, Haifa 32000, Israel

Received 22 August 2005; received in revised form 20 February 2006; accepted 1 June 2006
Available online 16 October 2006

Abstract

Annular plates are used in many engineering structures. In many cases variable thickness is used in order to save weight and improve structural characteristics. In recent years functionally graded materials (FGM) are used in many engineering applications. A FGM plate is an inhomogeneous composite made of two constituents (usually ceramic and metal), with both the composition and the material properties varying smoothly through the thickness of the plate. An optimal distribution of material properties may be obtained. The plate vibrations will have a strong bending–stretching coupling effect. The equations of motion including the effect of shear deformations using the first-order shear deformation theory are derived and solved exactly for various combinations of boundary conditions. The solution is obtained by using the exact element method. Exact vibration frequencies and modes are given for several examples for the first time.

1. Introduction

The problem of free transverse vibrations of isotropic annular plates is a well-known problem in structural dynamics. The comprehensive work of Leissa [1] covers fully the accumulated knowledge through the 1960s and the additional papers by the same author contain the updated work until the mid-1980s [2–7]. An extensive literature review of circular and annular plate vibrations dating back to the beginning of the 20th century was presented by Weisensel [8]. Irie et al. [9] presented exact solutions for the vibration frequencies of thick annular plates using Bessel functions. So and Leissa [10] used the Ritz method for three-dimensional (3D) vibration analysis of thick circular and annular plates. Liew and Yang [11] obtained elasticity solutions using orthogonally generated polynomial functions in the Ritz method. Liu and Lee [12] presented results from finite-element analysis for thick plates. Zhou et al. [13] used the Chebyshev–Ritz method to solve the problem. Duan et al. [14] gave exact solutions for thick annular plates vibrations.

The topic of variable thickness plates has recently been addressed by several methods. Many researches have used various formulations of the Ritz method to solve the problem approximately [15–18]. Shahab [19] and

*Corresponding author. Fax: +972 4 832 3433.
E-mail addresses: cvifraim@tx.technion.ac.il (E. Efraim), cvrmosh@tx.technion.ac.il (M. Eisenberger).

0022-460X/$ - see front matter
doi:10.1016/j.jsv.2006.06.068

Salmane and Lakis [20] presented finite-element solutions for nonuniform circular and annular plates. Shahab [19] also compared his solutions to experimental values obtained by using time-average holographic technique. Kang and Leissa [21] and Kang [22] used Ritz method for 3D analyses for linearly and nonlinearly thickness variation of annular plates, respectively. Eisenberger and Jabareen [23] presented exact solution for axi-symmetric vibrations of circular and annular plates with general polynomial variation of thickness. The differential quadrature method was utilized by Wang et al. [24], Laura et al. [25], and Wu and Liu [26], for approximate solution of circular and annular variable thickness plate vibrations. Duan et al. [27] used generalized hypergeometric function solutions for solving the problem and also presented comparison with finite-element model of variable thickness annular plate.

Functionally graded materials (FGM) were first introduced by material scientists in Japan in 1984 [28]. FGM are made by combining two different materials in such a way that their properties vary smoothly through the thickness of the plate. The use of FGM has many advantages in thermal environments and variation in their thickness can be utilized to reduce weight and achieve better vibrational behavior.

Reddy et al. [29] addressed the axisymmetric bending of functionally graded circular and annular plates. They solved only the static problem, and used a constant Poisson ratio through the thickness of the plate. They addressed only plates with constant thickness. In this paper, the vibration analysis of thick annular plates with variable thickness made of isotropic material and FGM are presented. The equations of motion are derived using a first-order shear deformation theory. The resulting equations of motion are highly coupled ordinary differential equations. For the variable thickness annular plate problem the equations have variable coefficients. The exact element method [30] is used to derive the exact frequency-dependent stiffness matrix for the plate. Then the natural frequencies are found as the values of the frequency that cause the dynamic stiffness matrix of the structure to become singular, and one can find as many frequencies as needed for design. Given the frequencies the exact modes of vibrations are found. Examples are given for the accuracy of the method and present the complex mode shapes of vibrations. The results for FGM plates are presented for the first time.

2. Basic equations

The five equation of motion for free vibration of the thick circular plate (Fig. 1) are obtained from the equations of motion of general shells [31], by substituting radiuses of curvature $R_s = \infty$ and $R_\theta = \infty$ and Lame parameters $A = 0$ and $B = s$, as

$$N_s(s,\theta) + s\frac{\partial N_s(s,\theta)}{\partial s} + \frac{\partial N_{\theta s}(s,\theta)}{\partial \theta} - N_\theta(s,\theta) + sq_s = 0, \tag{1a}$$

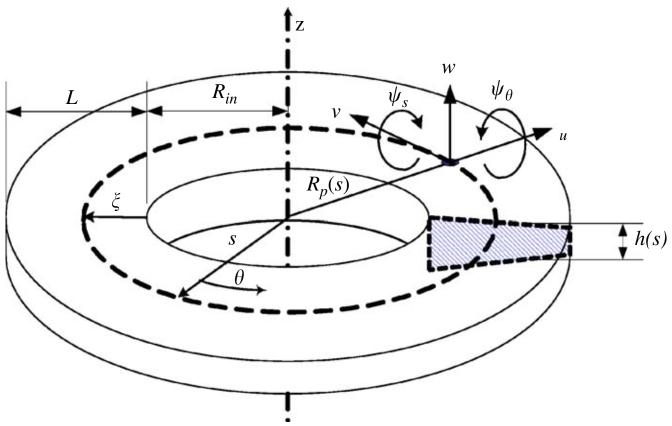

Fig. 1. Geometry, coordinate system and displacements of the annular circular plates with variation of thickness in the meridian direction.

$$\frac{\partial N_\theta(s,\theta)}{\partial \theta} + N_{s\theta}(s,\theta) + s\frac{\partial N_{s\theta}(s,\theta)}{\partial s} + N_{\theta s}(s,\theta) + sq_\theta = 0, \tag{1b}$$

$$Q_s(s,\theta) + s\frac{\partial Q_s(s,\theta)}{\partial s} + \frac{\partial Q_\theta(s,\theta)}{\partial \theta} + sq_z = 0, \tag{1c}$$

$$M_s(s,\theta) + s\frac{\partial M_s(s,\theta)}{\partial s} + \frac{\partial M_{\theta s}(s,\theta)}{\partial \theta} - M_\theta(s,\theta) - sQ_s(s,\theta) + sm_s = 0, \tag{1d}$$

$$\frac{\partial M_\theta(s,\theta)}{\partial \theta} + M_{s\theta}(s,\theta) + s\frac{\partial M_{s\theta}(s,\theta)}{\partial s} + M_{\theta s}(s,\theta) - sQ_\theta(s,\theta) + sm_\theta = 0, \tag{1e}$$

where the inertial forces and the rotary inertia moments are

$$q_s = -I_1(s)\frac{\partial^2 U(s,\theta,t)}{\partial t^2} - I_2(s)\frac{\partial^2 \Psi_s(s,\theta,t)}{\partial t^2}, \tag{2a}$$

$$q_\theta = -I_1(s)\frac{\partial^2 V(s,\theta,t)}{\partial t^2} - I_2(s)\frac{\partial^2 \Psi_\theta(s,\theta,t)}{\partial t^2}, \tag{2b}$$

$$q_z = -I_1(s)\frac{\partial^2 W(s,\theta,t)}{\partial t^2}, \tag{2c}$$

$$m_s = -I_2(s)\frac{\partial^2 U(s,\theta,t)}{\partial t^2} - I_3(s)\frac{\partial^2 \Psi_s(s,\theta,t)}{\partial t^2}, \tag{2d}$$

$$m_\theta = -I_2(s)\frac{\partial^2 V(s,\theta,t)}{\partial t^2} - I_3(s)\frac{\partial^2 \Psi_\theta(s,\theta,t)}{\partial t^2}. \tag{2e}$$

For FGM materials

$$I_1(s) = \int_{-h(s)/2}^{h(s)/2} \rho(z)\,\mathrm{d}z, \quad I_2(s) = \int_{-h(s)/2}^{h(s)/2} \rho(z)z\,\mathrm{d}z, \quad I_3(s) = \int_{-h(s)/2}^{h(s)/2} \rho(z)z^2\,\mathrm{d}z. \tag{3}$$

The force and moment resultants per unit length are obtained by integrating the stresses over the thickness of the plate as

$$\begin{bmatrix} N_s(s,\theta) \\ N_\theta(s,\theta) \\ N_{s\theta}(s,\theta) \\ N_{\theta s}(s,\theta) \end{bmatrix} = \int_{-h(s)/2}^{h(s)/2} \begin{bmatrix} \sigma_s \\ \sigma_\theta \\ \sigma_{s\theta} \\ \sigma_{\theta s} \end{bmatrix} \mathrm{d}z, \quad \begin{bmatrix} M_s(s,\theta) \\ M_\theta(s,\theta) \\ M_{s\theta}(s,\theta) \\ M_{\theta s}(s,\theta) \end{bmatrix} = \int_{-h(s)/2}^{h(s)/2} \begin{bmatrix} \sigma_s \\ \sigma_\theta \\ \sigma_{s\theta} \\ \sigma_{\theta s} \end{bmatrix} z\,\mathrm{d}z, \quad \begin{bmatrix} Q_s(s,\theta) \\ Q_\theta(s,\theta) \end{bmatrix} = \int_{-h(s)/2}^{h(s)/2} \begin{bmatrix} \sigma_{sz} \\ \sigma_{\theta z} \end{bmatrix} \mathrm{d}z. \tag{4}$$

The strain-displacement equations of the first-order shear deformation theory of thick circular plates are obtained by satisfying the Kirchoff–Love hypothesis, such that normal to the plate mid-surface during deformation remain straight, and suffer no extension, but are not necessarily normal to the mid-surface after deformation. According to these assumptions the displacement of every point of the plate may be expressed as

$$\begin{aligned} U(s,\theta,z,t) &= U_0(s,\theta,t) + z\Psi_s(s,\theta,t), \\ V(s,\theta,z,t) &= V_0(s,\theta,t) + z\Psi_\theta(s,\theta,t), \\ W(s,\theta,z,t) &= W_0(s,\theta,t) \end{aligned} \tag{5}$$

and the strains

$$\begin{aligned}
\varepsilon_s &= \varepsilon_{os} + zk_s,\\
\varepsilon_\theta &= \varepsilon_{o\theta} + zk_\theta,\\
\gamma_{s\theta} &= \gamma_{os\theta} + z\tau_{s\theta} + \gamma_{o\theta s} + z\tau_{\theta s},\\
\gamma_{sz} &= \gamma_{osz},\\
\gamma_{\theta z} &= \gamma_{o\theta z},
\end{aligned} \tag{6}$$

where

$$\left.\begin{aligned}
\varepsilon_{os} &= \frac{\partial}{\partial s}U_0(s,\theta,t), & \varepsilon_{o\theta} &= \frac{1}{s}\frac{\partial}{\partial\theta}V_0(s,\theta,t) + \frac{U_0(s,\theta,t)}{s},\\
k_s &= \frac{\partial}{\partial s}\Psi_s(s,\theta,t), & k_\theta &= \frac{1}{s}\frac{\partial}{\partial\theta}\Psi_\theta(s,\theta,t) + \frac{\Psi_s(s,\theta,t)}{s},\\
\gamma_{os\theta} &= \frac{\partial}{\partial s}V_0(s,\theta,t), & \gamma_{o\theta s} &= \frac{1}{s}\frac{\partial}{\partial\theta}U_0(s,\theta,t) - \frac{V_0(s,\theta,t)}{s},\\
\gamma_{osz} &= \frac{\partial}{\partial s}W_0(s,\theta,t) + \Psi_s(s,\theta,t), & \gamma_{o\theta z} &= \frac{1}{s}\frac{\partial}{\partial\theta}W_0(s,\theta,t) + \Psi_\theta(s,\theta,t),\\
\tau_{s\theta} &= \frac{\partial}{\partial s}\Psi_\theta(s,\theta,t), & \tau_{\theta s} &= \frac{1}{s}\frac{\partial}{\partial\theta}\Psi_s(s,\theta,t) - \frac{\Psi_\theta(s,\theta,t)}{s},
\end{aligned}\right] \tag{7}$$

are the strains and curvatures of the middle surface of the plate. For orthotropic materials the force and moment resultants obtained by integrating the stresses through the plate thickness, and for plates with variable thickness the constitutive relations become:

$$\begin{bmatrix} N_s(s,\theta)\\ N_\theta(s,\theta)\\ N_{s\theta}(s,\theta)\\ N_{\theta s}(s,\theta)\\ M_s(s,\theta)\\ M_\theta(s,\theta)\\ M_{s\theta}(s,\theta)\\ M_{\theta s}(s,\theta)\\ Q_s(s,\theta)\\ Q_\theta(s,\theta) \end{bmatrix}
= \begin{bmatrix}
A_{11}(s) & A_{12}(s) & 0 & 0 & B_{11}(s) & B_{12}(s) & 0 & 0 & 0 & 0\\
A_{12}(s) & A_{22}(s) & 0 & 0 & B_{12}(s) & B_{22}(s) & 0 & 0 & 0 & 0\\
0 & 0 & A_{66}(s) & A_{66}(s) & 0 & 0 & B_{66}(s) & B_{66}(s) & 0 & 0\\
0 & 0 & A_{66}(s) & A_{66}(s) & 0 & 0 & B_{66}(s) & B_{66}(s) & 0 & 0\\
B_{11}(s) & B_{12}(s) & 0 & 0 & D_{11}(s) & D_{12}(s) & 0 & 0 & 0 & 0\\
B_{11}(s) & B_{22}(s) & 0 & 0 & D_{12}(s) & D_{22}(s) & 0 & 0 & 0 & 0\\
0 & 0 & B_{66}(s) & B_{66}(s) & 0 & 0 & D_{66}(s) & D_{66}(s) & 0 & 0\\
0 & 0 & B_{66}(s) & B_{66}(s) & 0 & 0 & D_{66}(s) & D_{66}(s) & 0 & 0\\
0 & 0 & 0 & 0 & 0 & 0 & 0 & 0 & A_{55}(s) & 0\\
0 & 0 & 0 & 0 & 0 & 0 & 0 & 0 & 0 & A_{44}(s)
\end{bmatrix}
\begin{bmatrix} \varepsilon_{os}\\ \varepsilon_{o\theta}\\ \gamma_{os\theta}\\ \gamma_{o\theta s}\\ k_s\\ k_\theta\\ \tau_{s\theta}\\ \tau_{\theta s}\\ \gamma_{osz}\\ \gamma_{o\theta s} \end{bmatrix} \tag{8}$$

and the stiffness coefficients $A_{ij}(s)$, $B_{ij}(s)$, $D_{ij}(s)$ for plates made from functionally graded material are as follows:

$$\left.\begin{aligned} A_{ij}(s) &= \int_{-h(s)/2}^{h(s)/2} \overline{Q}_{ij}(z)\,\mathrm{d}z, \\ B_{ij}(s) &= \int_{-h(s)/2}^{h(s)/2} \overline{Q}_{ij}(z)z\,\mathrm{d}z, \\ D_{ij}(s) &= \int_{-h(s)/2}^{h(s)/2} \overline{Q}_{ij}(z)z^2\,\mathrm{d}z, \end{aligned}\right\} \quad (i,j = 1,2,6), \qquad \begin{aligned} \bar{Q}_{11}(z) &= \bar{Q}_{22}(z) = \frac{E(z)}{1-\mu(z)^2}, \\ \bar{Q}_{12}(z) &= \mu(z)\frac{E(z)}{1-\mu(z)^2}, \\ \bar{Q}_{44}(z) &= \bar{Q}_{55}(z) = \frac{E(z)}{2(1+\mu(z))}, \end{aligned}$$
$$A_{ii}(s) = \kappa \int_{-h(s)/2}^{h(s)/2} \overline{Q}_{ij}(z)\,\mathrm{d}z \quad (i = 4,5), \qquad \bar{Q}_{66}(z) = \frac{E(z)}{2(1+\mu(z))}. \tag{9}$$

Herein κ is the shear correction factor, and for FGM due to the variation of Poisson ratio through the thickness, is considered as

$$\kappa = \frac{5}{6 - \left(\mu_1 V_1 + \mu_2 V_2\right)}, \tag{10}$$

where V_1 and V_2 denotes the volume fraction of each material in the entire cross-section.

For FGM with two constituent materials the variations through the thickness of Young's modulus E, Poisson ratio μ, and the mass density ρ, can be expressed as

$$\begin{aligned} E(\bar{z}) &= (E_1 - E_2)V_f(\bar{z}) + E_2, \\ \rho(\bar{z}) &= (\rho_1 - \rho_2)V_f(\bar{z}) + \rho_2, \\ \mu(\bar{z}) &= (\mu_1 - \mu_2)V_f(\bar{z}) + \mu_2, \end{aligned} \tag{11}$$

where V_f is volume fraction of the top material, and it is assumed to follow a power-law distribution as

$$V_f(\bar{z}) = \left(\bar{z} + \frac{1}{2}\right)^g, \tag{12}$$

where $-1/2 \leqslant \bar{z} \leqslant 1/2$ is nondimensional coordinate through the thickness from the middle surface topward, and g is a gradient index.

For free harmonic vibrations of axisymmetric plates the displacement functions has been assumed as

$$\begin{aligned} U_0(s,\theta,t) &= u(s)\cos n\theta \sin \omega t, \\ V_0(s,\theta,t) &= v(s)\sin n\theta \sin \omega t, \\ W_0(s,\theta,t) &= w(s)\cos n\theta \sin \omega t, \\ \Psi_s(s,\theta,t) &= \psi_s(s)\cos n\theta \sin \omega t, \\ \Psi_\theta(s,\theta,t) &= \psi_\theta(s)\sin n\theta \sin \omega t. \end{aligned} \tag{13}$$

Substituting the displacement functions (13) and strain displacement relations (7) into Eqs. (8) and (1), and introducing the nondimensional meridian coordinate $0 \leqslant \xi \leqslant 1$

$$s = R_p(\xi) = R_{\mathrm{in}} + \xi L, \tag{14}$$

$$\frac{\partial}{\partial s}(\bullet) = \frac{1}{L}\frac{\partial}{\partial \xi}(\bullet) \tag{15}$$

yields the five differential equations of the motion for thick annular plates in terms of nondimensional coordinate ξ, for any value of the circumferential wave number n

$$\begin{aligned}&\left(R_p^2 I_2 \psi_s + R_p^2 I_1 u\right)\omega^2 + A_{11} f^2 u'' + \left(fA'_{11} + A_{11}\right) fu' + \left(fA'_{12} - A_{22} - A_{66} n^2\right) u \\ &\quad + (A_{12} + A_{66}) nfv' + \left(fA'_{12} - A_{22} - A_{66}\right) nv + B_{11} f^2 \psi''_s + \left(fB'_{11} + B_{11}\right) f\psi'_s \\ &\quad + \left(fB'_{12} - B_{22} - B_{66} n^2\right)\psi_s + (B_{12} + B_{66}) fn\psi'_\theta + \left(fB'_{12} - B_{22} - B_{66}\right) n\psi_\theta = 0,\end{aligned} \tag{16a}$$

$$\begin{aligned}&\left(R_p^2 I_2 \psi_t + R_p^2 I_1 v\right)\omega^2 - (A_{12} + A_{66}) fnu' - \left(fA'_{66} + A_{22} + A_{66}\right) nu + A_{66} f^2 v'' \\ &\quad + \left(A_{66} + fA'_{66}\right) fv' - \left(fA'_{66} + A_{22} n^2 + A_{66}\right) v - (B_{12} + B_{66}) fn\psi'_s \\ &\quad - \left(B_{22} + B_{66} + fB'_{66}\right) n\psi_s + B_{66} f^2 \psi''_\theta - (B_{12} + B_{66}) f\psi'_\theta - \left(fB'_{66} + B_{22} + B_{66}\right) n\psi_\theta = 0,\end{aligned} \tag{16b}$$

$$\begin{aligned}&R_p^2 I_1 w\omega^2 + A_{55} f^2 w'' + \left(fA'_{55} + A_{55}\right) fw' - A_{44} n^2 w \\ &\quad + R_p A_{55} f\psi'_s + R_p\left(fA'_{55} + A_{55}\right)\psi_s + R_p A_{44} n\psi_\theta = 0,\end{aligned} \tag{16c}$$

$$\begin{aligned}&\left(R_p^2 I_3 \psi_s + R_p^2 I_2 u\right)\omega^2 + B_{11} f^2 u'' + \left(fB'_{11} + B_{11}\right) fu' + \left(fB'_{12} - B_{22} - B_{66} n^2\right) u \\ &\quad + (B_{12} + B_{66}) nfv' + \left(fB'_{12} - B_{22} - B_{66}\right) nv - A_{55} R_p fw' + D_{11} f^2 \psi''_s + \left(fD'_{11} + D_{11}\right) f\psi'_s \\ &\quad + \left(fD'_{12} - D_{22} - D_{66} n^2\right)\psi_s + (D_{12} + D_{66}) fn\psi'_\theta + \left(fD'_{12} - D_{22} - D_{66}\right) n\psi_\theta = 0,\end{aligned} \tag{16d}$$

$$\begin{aligned}&(R_p^2 I_3 \psi_t + R_p^2 I_2 v)\omega^2 - (B_{12} + B_{66}) fnu' - \left(fB'_{66} + B_{22} + B_{66}\right) nu \\ &\quad + B_{66} f^2 v'' + \left(B_{66} + fB'_{66}\right) fv' - \left(fB'_{66} + B_{22} n^2 + B_{66}\right) v \\ &\quad + R_p A_{44} nw - (D_{12} + D_{66}) fn\psi'_s - \left(D_{22} + D_{66} + fD'_{66}\right) n\psi_s \\ &\quad + D_{66} f^2 \psi''_\theta + \left(D_{66} + fD'_{66}\right) f\psi'_\theta - \left(fD'_{66} + D_{22} n^2 + D_{66} + R_p^2 A_{44}\right)\psi_\theta = 0\end{aligned} \tag{16e}$$

and force and moment resultants along the circumference of the annular plate ($\xi = \text{const}$) are:

$$N_s = \left[\frac{A_{12}}{R_p} u + \frac{A_{11}}{L} u' + \frac{A_{12} n}{R_p} v + \frac{B_{11}}{L}\psi'_s + \frac{B_{12}}{R_p}\psi_s + \frac{B_{12} n}{R_p}\psi_\theta\right]\cos(n\theta)\sin(\omega t), \tag{17a}$$

$$N_{s\theta} = \left[-\frac{A_{66} n}{R_p} u + \frac{A_{66}}{L} v' - \frac{A_{66}}{R_p} v + \frac{B_{66}}{L}\psi'_\theta - \frac{B_{66} n}{R_p}\psi_s - \frac{B_{66}}{R_p}\psi_\theta\right]\sin(n\theta)\sin(\omega t), \tag{17b}$$

$$Q_s = \left[\frac{A_{55}}{L} w' + A_{55}\psi_s\right]\sin(n\theta)\sin(\omega t), \tag{17c}$$

$$M_s = \left[\frac{B_{12}}{R_p} u + \frac{B_{11}}{L} u' + \frac{B_{12} n}{R_p} v + \frac{D_{11}}{L}\psi'_s + \frac{D_{12}}{R_p}\psi_s + \frac{D_{12} n}{R_p}\psi_\theta\right]\cos(n\theta)\sin(\omega t), \tag{17d}$$

$$M_{s\theta} = \left[-\frac{B_{66} n}{R_p} u + \frac{B_{66}}{L} v' - \frac{B_{66}}{R_p} v + \frac{D_{66}}{L}\psi'_\theta - \frac{D_{66} n}{R_p}\psi_s - \frac{D_{66}}{R_p}\psi_\theta\right]\sin(n\theta)\sin(\omega t), \tag{17e}$$

where $(\bullet)' = \partial/\partial\xi$, $f = R_p(\xi)/L$ and all the coefficients A_{ij}, B_{ij}, D_{ij}, I_k, R_p, and f are functions of the coordinate ξ.

Table 1
Comparison of frequency parameters λ for constant thickness annular plates with free inner edge and various restrained outer edges (anti-symmetric thickness modes)

	h/R_o	R_i/R_o	Source of results	Mode types[a]					
				(0, 1)	(0, 2)	(1, 1)	(1, 2)	(2, 1)	(2, 2)
F–F	0.1	0.1	Ref. [9]	8.65	35.95	19.56	52.90	5.21	32.69
			Present I[b]	8.64687	35.95126	19.56464	52.89674	5.20623	32.69040
			Present II	8.65048	36.02964	19.59482	53.12031	5.20915	32.76966
			Ref. [11]	8.6518	36.036	19.596	53.148	5.2105	32.786
		0.3	Ref. [9]	8.23	46.63	17.02	52.5	4.8	30.77
			Present I	8.22690	46.63107	17.01848	52.50346	4.79545	30.76515
			Present II	8.22909	46.73297	17.05920	52.68111	4.79883	30.84624
			Ref. [11]	8.2291	46.730	17.063	52.693	4.7996	30.842
		0.5	Ref. [9]	9.10	81.03	15.76	83.48	4.17	28.05
			Present I	9.10194	81.03124	15.76240	83.47791	4.17100	28.04817
			Present II	9.10352	81.29307	15.80035	83.77901	4.17424	28.14113
			Ref. [11]	9.1036	81.306	15.783	83.770	4.173	28.085
	0.3	0.1	Ref. [9]	7.83	26.58	15.7	34.62	4.81	24.12
			Present I	7.83027	26.57574	15.69685	34.62412	4.80672	24.12241
			Present II	7.85231	26.83614	15.82308	35.14107	4.81956	24.37613
			Ref. [11]	7.8544	26.865	15.824	35.170	4.8172	24.403
		0.3	Ref. [9]	7.42	33.18	13.16	35.42	4.38	22.52
			Present I	7.41759	33.18240	13.15837	35.42176	4.38260	22.51570
			Present II	7.43018	33.45551	13.28114	35.78412	4.39686	22.77802
			Ref. [11]	7.4313	33.501	13.247	35.801	4.3921	22.758
		0.5	Ref. [9]	7.84	51.25	11.72	51.94	3.78	19.42
			Present I	7.84005	51.25196	11.72339	51.94135	3.78099	19.42135
			Present II	7.84710	51.70839	11.82027	52.43428	3.79611	19.65828
			Ref. [11]	7.8482	51.785	11.778	52.504	3.790	19.567
F–S	0.1	0.1	Ref. [9]	4.81	28.04	13.50	43.83	24.26	61.94
			Present I	4.81410	28.03666	13.45246	43.79495	24.06992	61.79552
			Present II	4.81577	28.09583	13.52093	44.00838	24.30692	62.24040
			Ref. [11]	4.8181	28.104	13.524	44.016	24.316	62.271
		0.3	Ref. [9]	4.63	34.92	12.19	41.45	23.07	57.18
			Present I	4.62960	34.91902	12.18902	41.44929	23.06717	57.18438
			Present II	4.63075	34.99520	12.21251	41.59770	23.11469	57.47651
			Ref. [11]	4.6329	35.002	12.208	41.582	23.116	57.445
		0.5	Ref. [9]	5.03	59.53	10.90	62.28	20.92	70.09
			Present I	5.03209	59.53088	10.90009	62.28302	20.92404	70.08873
			Present II	5.03296	59.73292	10.92275	62.52191	20.97814	70.43018
			Ref. [11]	5.0352	59.721	10.916	62.503	20.966	70.510
	0.3	0.1	Ref. [9]	4.54	21.67	11.5	30.05	19.04	39.93
			Present I	4.53849	21.66535	11.50426	30.05296	19.04346	39.93500
			Present II	4.55075	21.89698	11.59124	30.52570	19.24539	40.63137
			Ref. [11]	4.5572	21.933	11.602	30.565	19.279	40.757
		0.3	Ref. [9]	4.39	26.08	10.09	28.93	18.13	36.61
			Present I	4.38556	26.07791	10.08631	28.93210	18.12655	36.60536
			Present II	4.39392	26.33892	10.17374	29.29467	18.32447	37.21336
			Ref. [11]	4.4007	26.387	10.162	29.307	18.340	37.184
		0.5	Ref. [9]	4.72	39.22	8.94	40.24	16.11	43.25
			Present I	4.72052	39.21840	8.93782	40.23733	16.11157	43.25360
			Present II	4.72651	39.71663	9.00810	40.77474	16.29036	43.89833
			Ref. [11]	4.7367	39.798	8.990	40.836	16.256	42.972
F–C	0.1	0.1	Ref. [9]	9.90	36.33	20.04	52.53	31.86	71.35
			Present I	9.89625	36.32761	20.04205	52.53423	31.85782	71.34949
			Present II	9.91025	36.47405	20.09934	52.85596	31.98383	71.85394
			Ref. [11]	9.949	36.603	20.171	53.015	32.095	72.083
		0.3	Ref. [9]	11.12	46.25	18.12	51.74	30.08	66.24

Table 1 (*continued*)

h/R_o	R_i/R_o	Source of results	Mode types[a]					
			(0, 1)	(0, 2)	(1, 1)	(1, 2)	(2, 1)	(2, 2)
		Present I	11.12169	46.25268	18.12175	51.73694	30.07625	66.24395
		Present II	11.13662	46.48176	18.17963	52.04177	30.19470	66.72594
		Ref. [11]	11.18	46.641	18.220	52.173	30.266	66.828
	0.5	Ref. [9]	17.02	77.24	20.48	79.41	29.02	85.76
		Present I	17.02370	77.23862	20.48089	79.40782	29.01617	85.75651
		Present II	17.05562	77.85227	20.54137	80.05568	29.13922	86.50256
		Ref. [11]	17.142	78.150	20.614	80.339	29.197	86.748
0.3	0.1	Ref. [9]	8.37	24.7	15.01	32.23	22.02	41.64
		Present I	8.36584	24.70209	15.01476	32.23117	22.01586	41.64170
		Present II	8.44232	25.10690	15.22659	32.87114	22.37388	42.49528
		Ref. [11]	8.4771	25.203	15.274	32.982	22.461	42.734
	0.3	Ref. [9]	9.39	29.08	13.64	31.32	20.96	38.1
		Present I	9.38881	29.07770	13.63621	31.31832	20.95777	38.10000
		Present II	9.46958	29.57115	13.81758	31.88337	21.29719	38.85732
		Ref. [11]	9.5132	29.701	13.835	31.978	21.348	38.905
	0.5	Ref. [9]	13.55	40.9	15.42	41.71	20.21	44.29
		Present I	13.54754	40.89935	15.42158	41.70892	20.21069	44.28988
		Present II	13.69145	41.67399	15.61397	42.50513	20.51838	45.14628
		Ref. [11]	13.773	41.952	15.669	41.952	20.540	45.355

[a] The first number denotes the number of nodal diameters, whereas the second number indicates the order of the frequencies.
[b] I denotes the results of calculations with $\kappa = \pi^2/12$ whereas II denotes the results with $\kappa = 5/(6-\mu)$.

Table 2
Comparison of transverse natural frequencies (Hz) for linear variable thickness annular plates with clamped inner edge and free outer edges with experimental results and other methods

	Experiment [19]	Present analysis 21 DOF	Difference from experiment (%)	3D FE [19] 240 DOF	Difference from experiment (%)	Ritz 5-terms [19]	Difference from experiment (%)
$n = 0$	640	641.9	0.29	654	2.19	660	3.13
	—	2824.1	—	2865	—	2988	—
	—	7164.5	—	7238	—	7720	—
$n = 1$	580	581.4	0.25	591	1.90	595	2.59
	—	2921.7	—	2941	—	3088	—
	7338	7383.3	0.62	7416	1.06	7940	8.20
$n = 2$	663	691.9	4.35	670	1.06	698	5.28
	3311	3519.2	6.29	3457	4.41	3712	12.11
	7830	8332.9	6.42	8229	5.10	8900	13.67
$n = 3$	1152	1166.4	1.25	1111	−3.56	1238	7.47
	4529	4727.8	4.39	4589	1.32	5072	11.99
	9725	10159.1	4.46	9901	1.81	10850	11.57

3. Solution

The solution is assumed to be infinite polynomials in ξ, in the form

$$u(\xi) = \sum_{i=1}^{\infty} u_i \xi^i, \quad v(\xi) = \sum_{i=1}^{\infty} w_i \xi^i, \quad w(\xi) = \sum_{i=1}^{\infty} w_i \xi^i, \quad \psi_s(\xi) = \sum_{i=1}^{\infty} \psi_{si} \xi^i, \quad \psi_\theta(\xi) = \sum_{i=1}^{\infty} \psi_{\theta i} \xi^i. \tag{18}$$

Substitution of these proposed series solutions into the equations of motion, yields five recurrence formulas for the terms u_{i+2}, v_{i+2}, w_{i+2}, $\psi_{s_{i+2}}$ and $\psi_{\theta_{i+2}}$ as in the exact element method [30]. Then following the same procedure as in Ref. [30] the particular solutions for unit displacement in the five degrees of freedom at each of the two edges of the annular plate (radial displacement, circumferential displacement, transverse displacement, and the two rotations about the circumference and radius of the plate), are used to find the dynamic stiffness terms which are the end forces and moments due to unit displacements. For each mode shape one has the five end forces, or stiffnesses along the unit angle segment of the perimeter of the

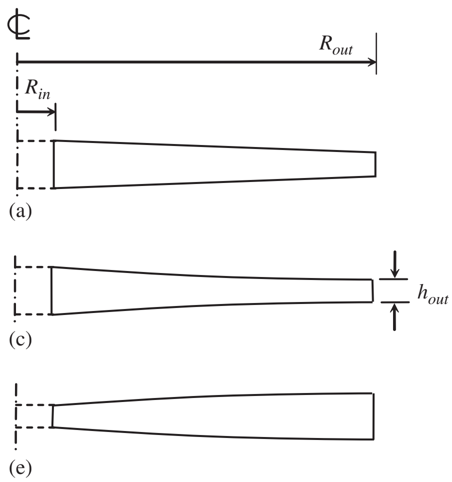

Fig. 2. Types of variation of the plate thickness: (a, b) linear form; (c, d) quadratically concave form; and (e, f) quadratically convex form.

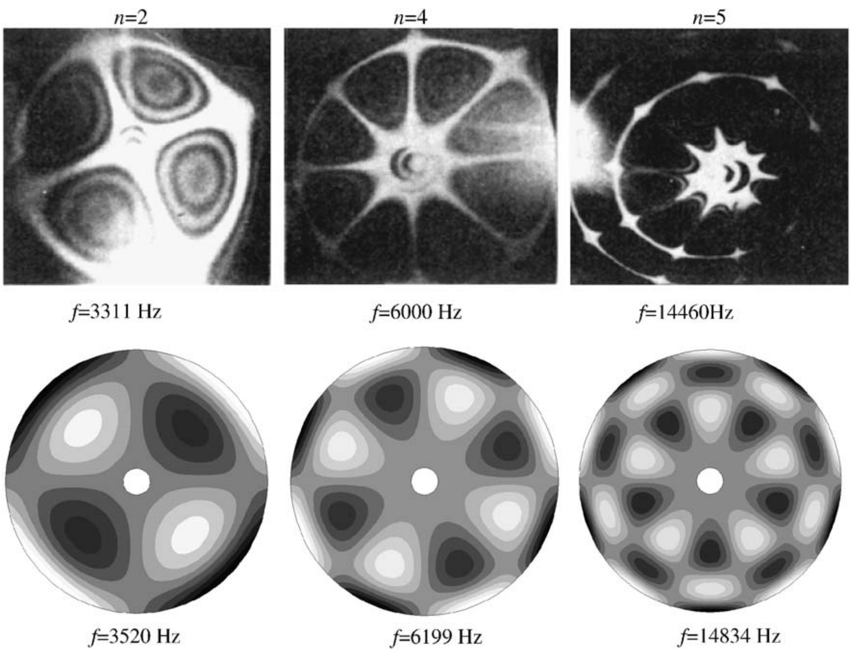

Fig. 3. Vibration frequencies and mode shapes of tapered disk: (a) experimental laser holograms [19]; and (b) shapes obtained by present study (contour plots).

plate edges, as follows:

$$\left.\begin{matrix} S_1 \\ S_6 \end{matrix}\right\} = N_s = \left[A_{12}u + fA_{11}u' + A_{12}nv + fB_{11}\psi_s' + B_{12}\psi_s + B_{12}n\psi_\theta\right]\Big|\begin{matrix}\xi = 0, \\ \xi = 1,\end{matrix} \tag{19a}$$

$$\left.\begin{matrix} S_2 \\ S_7 \end{matrix}\right\} = N_\theta = \left[-A_{66}nu + fA_{66}v' - A_{66}v + fB_{66}\psi_\theta' - B_{66}n\psi_s - B_{66}\psi_\theta\right]\Big|\begin{matrix}\xi = 0, \\ \xi = 1,\end{matrix} \tag{19b}$$

$$\left.\begin{matrix} S_3 \\ S_8 \end{matrix}\right\} = Q_s = \left[fA_{55}w' + R_pA_{55}\psi_s\right]\Big|\begin{matrix}\xi = 0, \\ \xi = 1,\end{matrix} \tag{19c}$$

$$\left.\begin{matrix} S_4 \\ S_9 \end{matrix}\right\} = M_s = \left[B_{12}u + fB_{11}u' + B_{12}nv + fD_{11}\psi_s' + D_{12}\psi_s + D_{12}n\psi_\theta\right]\Big|\begin{matrix}\xi = 0, \\ \xi = 1,\end{matrix} \tag{19d}$$

$$\left.\begin{matrix} S_5 \\ S_{10} \end{matrix}\right\} = M_{s\theta} = \left[-B_{66}nu + fB_{66}v' - B_{66}v + fD_{66}\psi_\theta' - D_{66}n\psi_s - D_{66}\psi_\theta\right]\Big|\begin{matrix}\xi = 0, \\ \xi = 1.\end{matrix} \tag{19e}$$

Table 3
Comparison of transverse natural frequencies (Hz) for linear increasing variable thickness annular plates ($h(s) = s/15$) with clamped inner and free outer edges with 3D finite-element solution and generalized hypergeometric function [27]

		C–C					F–C				
		3D-FEM	Present	%	Duan et al. [27]	%	3D-FEM	Present	%	Duan et al. [27]	%
$n = 0$	1	223.46	220.475	−1.34	223.772	0.14	149.25	148.882	−0.25	149.603	0.24
	2	580.01	571.054	−1.54	582.352	0.40	382.44	381.146	−0.34	385.354	0.76
	3	1097.6	1077.93	−1.79	1114.61	1.55	750.72	747.171	−0.47	762.903	1.62
$n = 1$	1	258.17	255.616	−0.99	258.972	0.31	218.33	217.765	−0.26	219.379	0.48
	2	618.09	609.675	−1.36	622.285	0.68	468.7	467.029	−0.36	473.471	1.02
	3	1136.6	1117.65	−1.67	1156.68	1.77	833.16	829.009	−0.50	848.42	1.83
$n = 2$	1	363.45	361.552	−0.52	366.295	0.78	352.45	351.432	−0.29	355.647	0.91
	2	737.36	730.307	−0.96	747.363	1.36	665.41	663.004	−0.36	675.195	1.47
	3	1257.9	1240.89	−1.35	1287.40	2.35	1055.9	1050.64	−0.50	1079.5	2.24

Table 4
Comparison of transverse natural frequencies (Hz) for nonlinear increasing variable thickness annular plates ($h(s) = 1/15\sqrt{s}$) with clamped inner and free outer edges with 3D finite-element solution and generalized hypergeometric function [27]

		C–C					F–C				
		3D-FEM	Present	%	Duan et al. [27]	%	3D-FEM	Present	%	Duan et al. [27]	%
$n = 0$	1	302.12	300.045	−0.69	306.027	1.29	153.21	152.791	−0.27	153.859	0.42
	2	821.29	814.109	−0.87	849.045	3.38	491.62	489.749	−0.38	499.91	1.69
	3	1573.40	1555.934	−1.11	1669.238	6.09	1044.4	1038.440	−0.57	1081.78	3.58
$n = 1$	1	336.99	334.891	−0.62	342.054	1.50	273.71	272.897	−0.30	276.75	1.11
	2	869.35	862.050	−0.84	900.462	3.58	670.37	667.603	−0.41	688.64	2.73
	3	1626.60	1608.944	−1.09	1728.966	6.29	1229	1221.551	−0.61	1286.28	4.66
$n = 2$	1	459.55	457.348	−0.48	468.545	1.96	444.78	443.130	−0.37	452.562	1.75
	2	1027.20	1019.540	−0.75	1069.060	4.08	956.33	951.464	−0.51	989.164	3.43
	3	1797.40	1779.010	−1.02	1919.878	6.81	1610.1	1599.240	−0.67	1699.11	5.53

Table 5
Comparison of nondimensional frequencies in $\omega R_{\mathrm{out}}\sqrt{\rho/G}$ of completely free, tapered annular plates

n	$p = 1$, $h_{\mathrm{out}}/h_{\mathrm{in}} = 1/4$, $h_{\mathrm{in}}/R_{\mathrm{out}} = 1/6$				$p = 1$, $h_{\mathrm{out}}/h_{\mathrm{in}} = 4$, $h_{\mathrm{in}}/R_{\mathrm{out}} = 1/24$				$p = 2$, $h_{\mathrm{out}}/h_{\mathrm{in}} = 1/4$, $h_{\mathrm{in}}/R_{\mathrm{out}} = 1/6$				$p = 2$, $h_{\mathrm{out}}/h_{\mathrm{in}} = 4$, $h_{\mathrm{in}}/R_{\mathrm{out}} = 1/24$			
	Kang [22]	Present study		Diff. %	Kang [22]	Present study		Diff. %	Kang [22]	Present study		Diff. %	Kang [22]	Present study		Diff. %
0	1.098	L	1.0882	−0.89	0.7611	L	0.7630	0.25	1.276	L	1.2634	−0.98	0.6343	L	0.6350	0.11
	3.405	L	3.3992	−0.17	2.729	R	2.7317	0.10	3.555	R	3.5786	0.67	2.296	L	2.3060	0.44
	3.643	R	3.6671	0.66	3.186	L	3.1819	−0.13	4.091	L	4.0747	−0.40	2.641	R	2.6426	0.06
	6.503	L	6.4932	−0.15	6.293	L	6.2668	−0.42	7.419	L	7.3892	−0.40	5.042	L	5.0486	0.13
	8.157	R	8.2463	1.09	8.261	R	8.3895	1.56	8.301	R	8.4691	2.02	8.217	L	8.2658	0.59
0	4.984	T	5.0029	0.38	5.637	T	5.6583	0.38	5.185	T	5.2108	0.50	5.655	T	5.6827	0.49
	8.488	T	8.5211	0.39	9.022	T	9.0556	0.37	8.657	T	8.6982	0.48	8.864	T	8.9055	0.47
	12.030	T	12.0769	0.39	10.560	Tr	10.8027	2.30	11.160	Tr	11.3469	1.67	11.200	Tr	11.3615	1.44
	12.390	Tr	12.5137	1.00	12.450	T	12.5012	0.41	12.160	T	12.2218	0.51	12.280	T	12.3398	0.49
	15.640	T	15.6957	0.36	15.320	Tr	15.7659	2.91	13.860	Tr	14.0745	1.55	15.820	T	15.8955	0.48
1	1.969	OP	1.9676	−0.07	1.489	OP	1.4901	0.07	2.360	OP	2.3458	−0.60	1.188	OP	1.1905	0.21
	2.928	IP	2.9329	0.17	2.734	IP	2.7360	0.07	2.970	IP	2.9763	0.21	2.683	IP	2.6845	0.06
	4.249	OP	4.2563	0.17	3.796	OP	3.7864	−0.25	4.859	OP	4.8511	−0.16	2.926	OP	2.9348	0.30
	6.647	IP	6.7344	1.31	6.585	IP	6.6558	1.07	6.776	IP	6.9032	1.88	5.474	OP	5.4767	0.05
	6.868	IP	6.8901	0.32	6.691	OP	6.6568	−0.51	7.022	IP	7.0730	0.73	6.390	IP	6.4467	0.89
2	0.650	OP	0.6490	−0.20	0.4932	OP	0.4960	0.56	0.7626	OP	0.7600	−0.34	0.4116	OP	0.4147	0.74
	2.370	IP	2.3763	0.27	1.621	IP	1.6230	0.13	2.297	IP	2.2962	−0.03	1.542	IP	1.5448	0.18
	2.924	OP	2.9162	−0.27	2.649	OP	2.6515	0.09	3.536	OP	3.5103	−0.73	2.129	OP	2.1348	0.27
	4.233	IP	4.2414	0.20	4.044	IP	4.0476	0.09	4.289	IP	4.3009	0.28	4.008	IP	4.0111	0.08
	5.750	OP	5.7355	−0.25	5.127	OP	5.1122	−0.29	6.477	OP	6.4525	−0.38	4.163	OP	4.1741	0.27
3	1.200	OP	1.1959	−0.34	1.242	OP	1.2511	0.73	1.492	OP	1.4834	−0.57	1.071	OP	1.0813	0.96
	3.960	OP	3.9492	−0.27	3.040	IP	3.0524	0.41	4.159	IP	4.1653	0.15	2.848	IP	2.8614	0.47
	4.217	IP	4.2283	0.27	3.899	OP	3.9016	0.07	4.682	OP	4.6556	−0.56	3.224	OP	3.2325	0.26
	6.000	IP	6.0095	0.16	5.679	IP	5.6916	0.22	6.043	IP	6.0614	0.30	5.512	OP	5.5158	0.07
	7.067	OP	7.0419	−0.36	6.594	OP	6.5702	−0.36	7.894	OP	7.8533	−0.52	5.645	IP	5.6548	0.17

The natural frequencies of vibrations are found as the values of ω that cause the stiffness matrix of the plate, taking into account the external restraints, to become singular. Then, a simple search method is used to converge on all the natural frequencies, for any value of n.

Table 6
Properties of FGM components at temperature $T = 300\,\mathrm{K}$

Material	Properties		
	Young's modulus, E ($\mathrm{N/m^2}$)	Poisson ratio, μ	Density, ρ ($\mathrm{kg/m^3}$)
Stainless steel SUS304	207,787,700,000	0.317756	8166
Silicon nitride Si3N4	322,271,500,000	0.24	2370

Table 7
Natural frequencies $\Omega = \omega R_{\mathrm{out}}\sqrt{\rho_{\mathrm{st}}/E_{\mathrm{st}}}$ of free-free FGM (Si_3N_4-SUS304) annular disc with variable thickness ($g = 1$, $R_{\mathrm{in}}/R_{\mathrm{out}} = 0.2$, $H/R_{\mathrm{out}} = 0.1$)

		$n = 0$	$n = 1$	$n = 2$	$n = 3$	$n = 4$	$n = 5$
Linear thickness variation (a-type)							
1	L	0.3781	0.8226	0.2262	0.5030	0.8350	1.2270
2	L	1.6616	2.1471	1.3619	1.9994	2.6810	3.3953
3	E	2.7545	2.4714	1.7404	3.2471	4.2991	5.2060
4	L	3.7599	4.0963	3.0348	3.9505	4.8827	5.8097
5	T	4.5057	5.6528	3.5822	5.0684	6.5389	7.9390
6	L	6.4377	6.1851	5.0241	6.1601	7.2931	8.3885
7	E	6.9732	6.6753	5.8813	6.9926	8.7042	10.1745
8	T	7.6842	9.1435	7.3794	8.4992	9.7723	11.0173
9	L	9.4749	9.6389	7.6564	9.3313	10.8054	12.3442
10	T	10.9377	10.7744	9.8853	10.4166	11.6822	13.4351
Parabolic thickness variation (convex f-type)							
1	L	0.4048	0.8865	0.2433	0.5452	0.9020	1.3171
2	L	1.8058	2.2888	1.4711	2.1461	2.8666	3.6183
3	E	2.7470	2.4890	1.7301	3.2533	4.3299	5.2543
4	L	4.0122	4.3410	3.2167	4.1783	5.1509	6.1158
5	T	4.5647	5.7285	3.6047	5.0867	6.5579	7.9601
6	L	6.7654	6.2333	5.2646	6.4323	7.6052	8.7354
7	E	7.0655	7.0064	5.9679	7.0469	8.7162	10.1698
8	T	7.7296	9.1835	7.6803	8.8084	10.1030	11.3803
9	L	9.8682	10.0288	7.7018	9.3664	10.8421	12.3668
10	T	10.9703	10.8176	9.9250	10.4509	11.7120	13.4536
Parabolic thickness variation (concave c-type)							
1	L	0.3647	0.7898	0.2177	0.4822	0.8019	1.1824
2	L	1.5896	2.0755	1.3066	1.9251	2.5863	3.2806
3	E	2.7583	2.4618	1.7457	3.2427	4.2811	5.1783
4	L	3.6302	3.9706	2.9404	3.8318	4.7424	5.6485
5	T	4.4733	5.6095	3.5701	5.0588	6.5289	7.9270
6	L	6.2630	6.1608	4.8991	6.0161	7.1271	8.2039
7	E	6.9260	6.5021	5.8342	6.9632	8.6983	10.1782
8	T	7.6609	9.1217	7.2132	8.3351	9.5944	10.8208
9	L	9.2650	9.4315	7.6410	9.3129	10.7863	12.3326
10	T	10.9212	10.7529	9.8517	10.3994	11.6672	13.4201

E—Extensional mode of vibration with dominant radial oscillations.
L—Vibration mode with dominant lateral oscillations.
T—Torsional mode of vibration.

4. Examples

For verification of the present formulation, a comparison study of the results for thick annular plates with constant thickness, and F–F, S–F, and C–F boundary conditions, is made with the results from Mindlin theory given by Irie et al. [9], and with the 3D elasticity analysis by Liew and Yang [11]. These are presented in Table 1. The boundary conditions are: F–F: free both in the inner and outer radius, F–S: free on the inner radius and simply supported on the outer, and F–C: free on the inner radius and clamped on the outer radius. The results are given in terms of the nondimensional frequency parameter $\lambda = \omega R_{\text{out}}^2\sqrt{12(1-\mu^2)\rho/E}/(2\pi h)$. The results are exactly the same as in Ref. [9], and lower than the results of Ref. [11]; the reason the current solution is softer than the 3D solution is that the warping of the cross section is relaxed in the current kinematics relationships.

In Table 2 a comparison is shown between the transverse natural frequencies for a linearly tapered clamped-free disc made of steel that were obtained by the present analysis (type (a) in Fig. 2), and the experimental and theoretical results that were presented by Shahab [19]. The geometrical parameters are $R_{\text{in}}/R_{\text{out}} = 0.1$,

Table 8

Natural frequencies $\Omega = \omega R_{\text{out}}\sqrt{\rho_{\text{st}}/E_{\text{st}}}$ of free–free FGM (Si_3N_4-SUS304) annular disc with variable thickness ($g = 5$, $R_{\text{in}}/R_{\text{out}} = 0.2$, $H/R_{\text{out}} = 0.1$)

		$n=0$	$n=1$	$n=2$	$n=3$	$n=4$	$n=5$
Linear thickness variation (a-type)							
1	L	0.3110	0.6744	0.1839	0.4092	0.6795	0.9987
2	L	1.3625	1.7536	1.1175	1.6375	2.1925	2.7735
3	E	2.2027	1.9506	1.3691	2.5479	3.3737	4.0870
4	L	3.0777	3.3452	2.4801	3.2277	3.9837	4.7336
5	T	3.5300	4.5088	2.8219	3.9947	5.1536	6.2530
6	L	5.2559	4.8558	4.0896	5.0128	5.9312	6.8132
7	E	5.5405	5.4432	4.6642	5.5268	6.8600	8.0137
8	T	6.0211	7.1878	6.0000	6.8924	7.9185	8.9216
9	L	7.7129	7.8418	6.0685	7.4079	8.5549	9.7612
10	T	8.5726	8.5211	7.7619	8.1945	9.2233	10.6105
Parabolic thickness variation (convex f-type)							
1	L	0.3329	0.7264	0.1979	0.4435	0.7339	1.0718
2	L	1.4804	1.8688	1.2068	1.7573	2.3436	2.9545
3	E	2.1962	1.9649	1.3612	2.5528	3.3978	4.1250
4	L	3.2824	3.5437	2.6267	3.4114	4.1995	4.9790
5	T	3.5762	4.5654	2.8398	4.0087	5.1678	6.2682
6	L	5.5084	4.8964	4.2828	5.2291	6.1787	7.0879
7	E	5.6247	5.7093	4.7319	5.5700	6.8705	8.0113
8	T	6.0569	7.2188	6.0919	7.1373	8.1773	9.2045
9	L	8.0245	8.1510	6.2549	7.4370	8.5852	9.7796
10	T	8.5988	8.5552	7.7900	8.2214	9.2475	10.6272
Parabolic thickness variation (concave c-type)							
1	L	0.3001	0.6477	0.1770	0.3923	0.6526	0.9625
2	L	1.3036	1.6953	1.0722	1.5767	2.1152	2.6802
3	E	2.2060	1.9429	1.3733	2.5444	3.3596	4.0654
4	L	2.9722	3.2431	2.4039	3.1319	3.8705	4.6040
5	T	3.5046	4.4758	2.8122	3.9874	5.1463	6.2450
6	L	5.1161	4.8361	3.9891	4.8980	5.7991	6.6659
7	E	5.5020	5.3033	4.6274	5.5034	6.8548	8.0160
8	T	6.0027	7.1714	5.8670	6.7622	7.7788	8.7678
9	L	7.5461	7.6763	6.0552	7.3927	8.5391	9.7518
10	T	8.5594	8.5042	7.7474	8.1813	9.2112	10.6018

E—Extensional mode of vibration with dominant radial oscillations.
L—Vibration mode with dominant lateral oscillations.
T—Torsional mode of vibration.

$h_{in}/h_{out} = 3$, $R_{out} = 3.5$ in (0.089 m), $h_{in} = 3/16$ in (0.00476 m), and the material properties are $\rho = 0.285\,\text{lb/in}^3$ ($7888\,\text{kg/m}^3$), $E = 30 \times 10^6\,\text{lbf/in}^2$ ($2.06913 \times 10^{11}\,\text{N/m}^2$), and $\mu = 0.3$. In Ref. [19] the Ritz five-term approach and a thick 3D cylindrical finite element with 96 degrees of freedom, were used for the calculations of the frequencies of tapered disc. For low number of circumferential waves the present results are closer to the experimental results, and in general are higher, whereas the 3D FEM solution gives in some cases values that are lower than the experimental frequencies. The experimental results of Shahab [19] are compared with the current solution, together with the mode shapes in Fig. 3. The frequency values are very close to the experimental values, and the modes are identical.

Another comparison for linear and nonlinear variation of isotropic plates clamped at the inner edge and free at the outer edge was presented by Duan et al. [27]. In Table 3 results are given for linearly increasing thickness

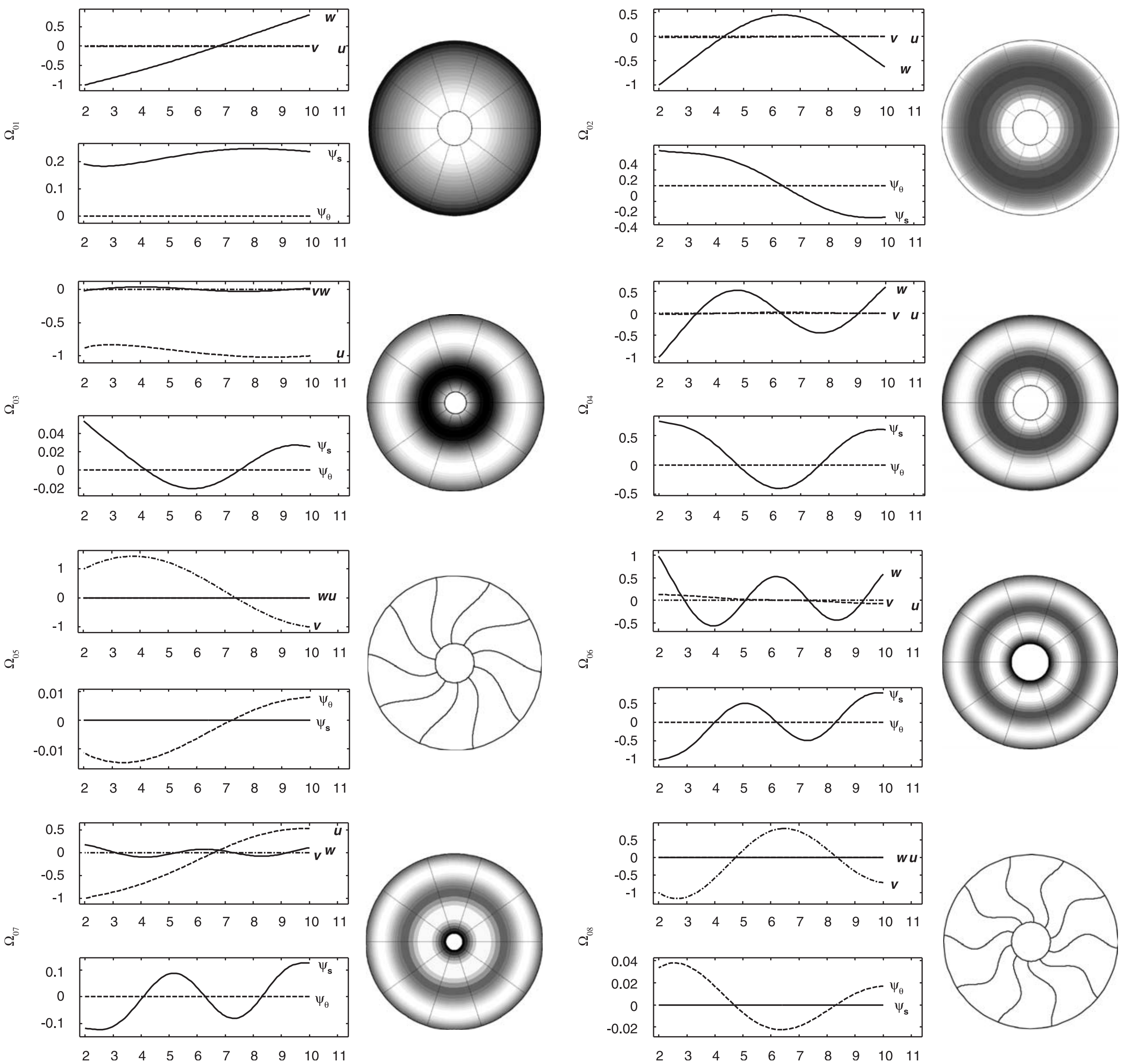

Fig. 4. Mode shapes of vibrations of completely free FGM annular plate with parabolic concave variable thickness ($g = 5$, $n = 0, 1$). For each mode, the upper plot shows displacement amplitudes u (dashed line), v (chain-dotted line), w (solid line), the lower plot shows displacement amplitudes ψ_θ (dashed line), and ψ_s (solid line).

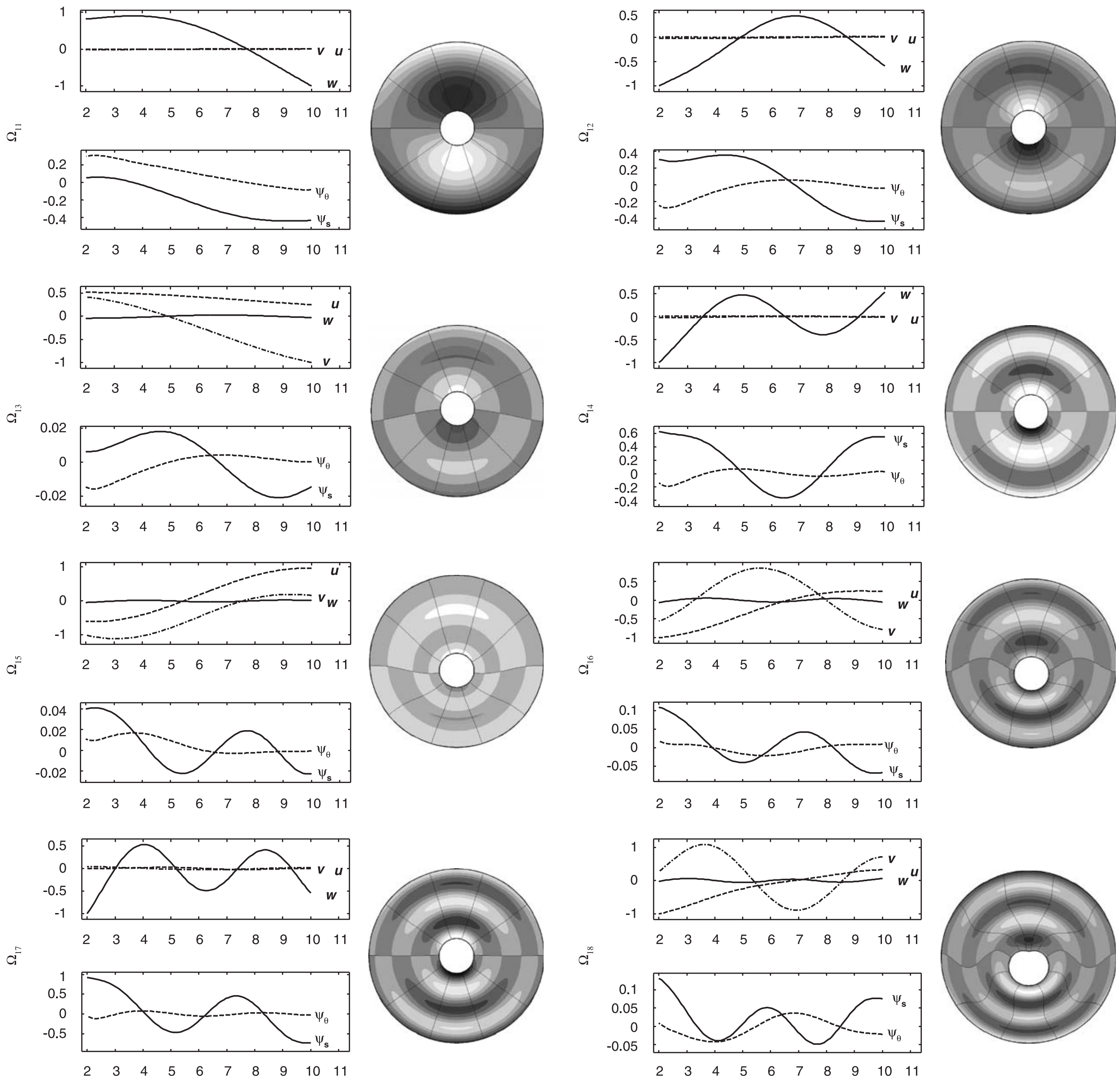

Fig. 4. (*Continued*)

annular plate ($h(s) = s/15$, type (b) in Fig. 2). The FE model was constructed using 1242 3D elements. In Table 4 plates with nonlinear increasing variation of thickness ($h(s) = s^{0.5}/15$, type (e) in Fig. 2) are compared with 3195 3D elements FE model. The present results are very close to both the numerical FEM values and the results that were obtained by the generalized hypergeometric functions method.

Table 5 presents the nondimensional frequencies of completely free annular plates with radius ratio $R_{in}/R_{out} = 1/6$, $\mu = 0.3$ and different types of thickness variation that are expressed as follows:

$$h(\xi) = h_{in}\left(1 + \xi^p\left(h_{out}/h_{in} - 1\right)\right), \tag{20}$$

where p represents the characteristics of the variation: $p = 1$ for linear variation, and $p = 2$ for parabolic variation. The results are compared with those given by Kang [22] that obtained by 3D Ritz analysis.

The results are presented with indication of the vibrational mode type as follows: for axisymmetric vibrations, $n = 0$, the letter L stands for lateral vibration modes, R for radial modes, T for torsional modes, and Tr for torsional modes about the radius, which represent opposite in-plane motion of the upper part of the plate, relative to the motion of the bottom part. For higher wave numbers ($n > 0$), the modes are coupled, and are identified as out-of-plane modes (OP), and in-plane modes (IP). It can be seen that for most of the lateral and OP the results that are obtained using the current method yield lower upper bound values for the frequency than the reference values from Ref. [22]. For in-plane motions the present results are slightly higher than those from Ref. [22].

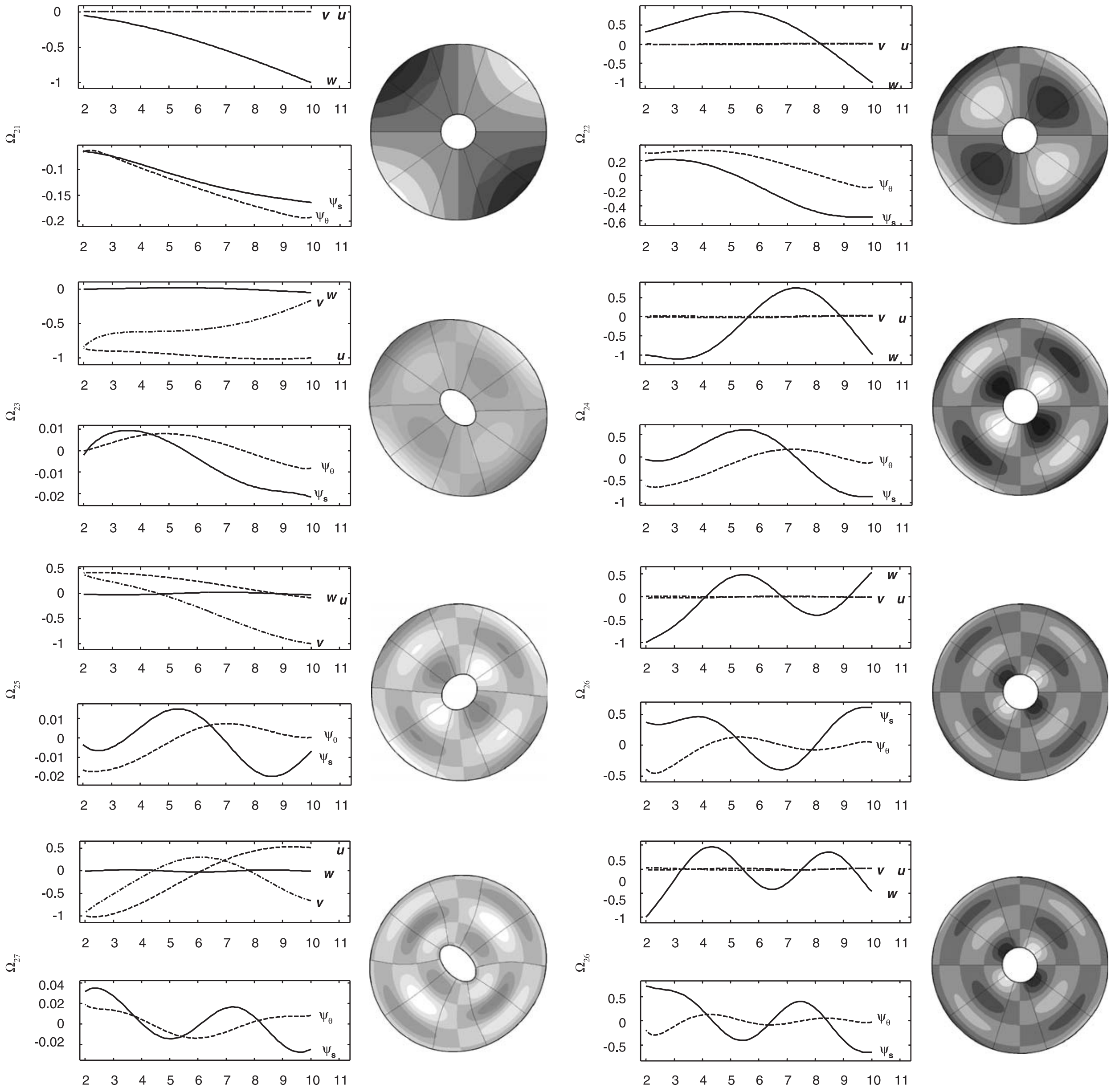

Fig. 5. Mode shapes of vibrations of completely free FGM annular plate with parabolic concave variable thickness ($g = 5$, $n = 2, 3$). For each mode, the upper plot shows displacement amplitudes u (dashed line), v (chain-dotted line), w (solid line), the lower plot shows displacement amplitudes ψ_θ (dashed line), and ψ_s (solid line).

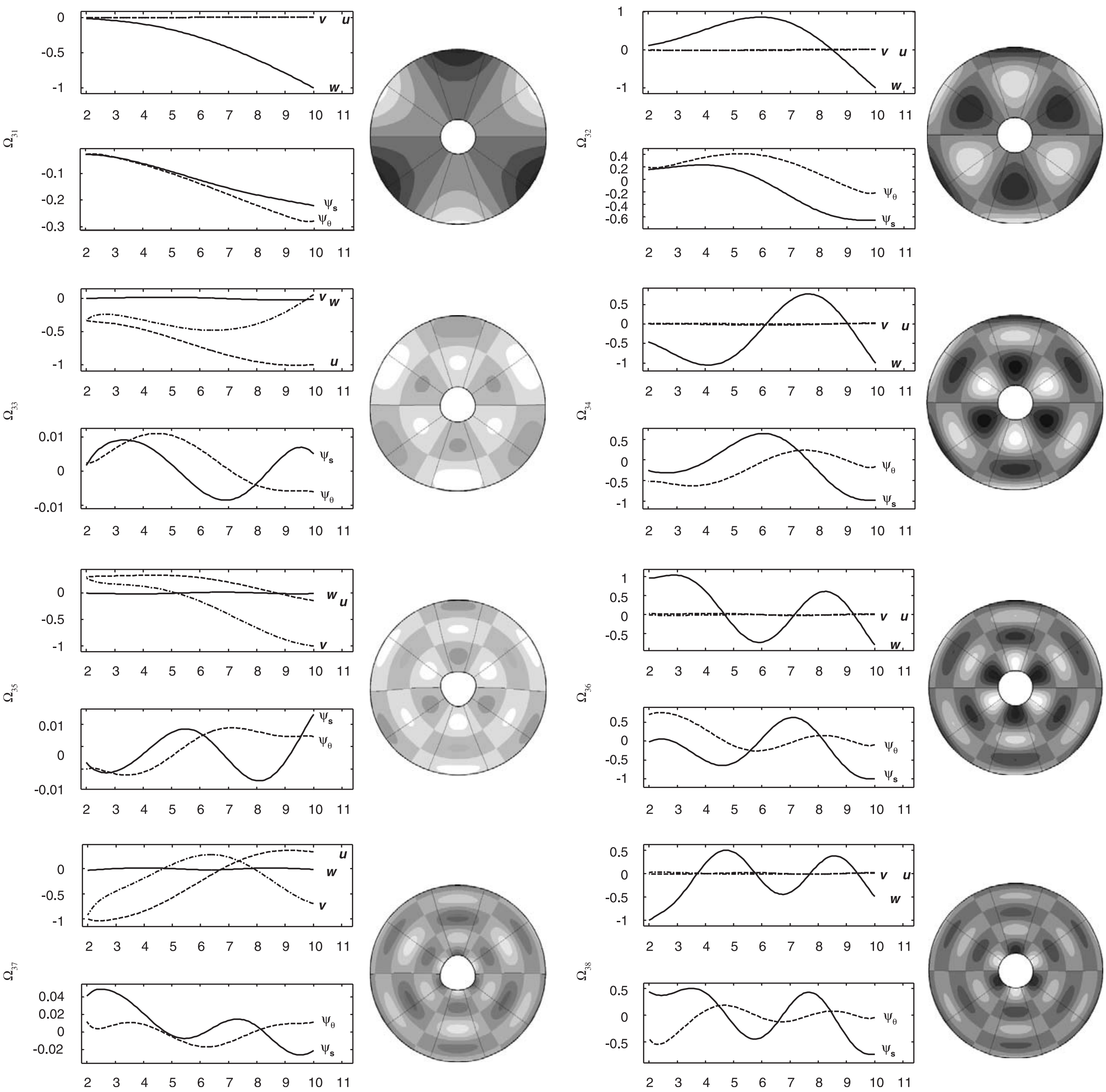

Fig. 5. (*Continued*)

Results for FGM plates are given here for the first time. The material properties are given in Table 6 and the results for two gradient indexes are given in Table 7 ($g = 1$), and Table 8 ($g = 5$). A completely free silicone-nitride-stainless steel annular disc with variable thickness was analyzed. The upper surface is made from silicone-nitride. The radius ratio is $R_{\mathrm{in}}/R_{\mathrm{out}} = 0.2$, and thickness to radius ratio $H/R_{\mathrm{out}} = 0.1$. Three types of thickness variations were examined:

(a) $h(\xi) = H(1.2{-}0.4\xi)$ or $h(\overline{\xi}) = H\left(0.8 + 0.4\overline{\xi}\right)$ for linear variation (type (*a*) in Fig. 2);

(b) $h(\xi) = H(1.2{-}0.4\xi^2)$ or $h(\overline{\xi}) = H\left(0.8 + 0.8\overline{\xi} - 0.4\overline{\xi}^2\right)$ for convex variation (type (*f*) in Fig. 2);

(c) $h(\xi) = H(1.2{-}0.6\xi + 0.2\xi^2)$ or $h(\overline{\xi}) = H\left(0.8 + 0.4\overline{\xi}^2\right)$ for concave variation (type (*c*) in Fig. 2).

Results for the first 10 natural dimensionless frequencies $\Omega = \omega R_{\text{out}} \sqrt{\rho_{\text{st}}/E_{\text{st}}}$ are given in the tables for six circumferential wave numbers ($n = 0, 1, \ldots, 5$). Figs. 4 and 5 present the mode shape functions and contour plots for the first eight frequencies in each sequence, for circumferential wave numbers $n = 0$, 1, 2, 3. The present data of the free vibration of FGM annular thick plates may be regarded as benchmark results for comparison with other methods.

5. Conclusions

The exact free vibration frequencies and modes of variable thickness thick annular plates, made of isotropic and functionally graded materials (FGM) are found. The resulting system of equations of motion is a coupled set of partial differential equations with variable coefficients, and the exact solution is obtained using the exact element method and the dynamic stiffness method. Results for variable thickness thick FGM plates are given for the first time, and it is hoped that these can serve as reference values for other computational methods.

References

[1] A.W. Leissa, *Vibrations of Plates*, NASA SP-160, USA, 1969.

[2] A.W. Leissa, Recent research in plate vibrations: classical theory, *The Shock and Vibration Digest* 9 (1977) 13–24.

[3] A.W. Leissa, Recent research in plate vibrations, 1973–1976: complicating effects, *The Shock and Vibration Digest* 10 (1978) 21–35.

[4] A.W. Leissa, Plate vibration research, 1976–1980: classical theory, *The Shock and Vibration Digest* 13 (1981) 11–22.

[5] A.W. Leissa, Plate vibration research, 1976–1980: complicating effects, *The Shock and Vibration Digest* 13 (1981) 19–36.

[6] A.W. Leissa, Recent studies in plate vibrations: 1981–1985, Part I: classical theory, *The Shock and Vibration Digest* 19 (1987) 11–18.

[7] A.W. Leissa, Recent studies in plate vibrations: 1981–1985, Part II: complicating effects, *The Shock and Vibration Digest* 19 (1987) 10–24.

[8] G.N. Weisensel, Natural frequency information for circular and annular plates, *Journal of Sound and Vibration* 133 (1989) 129–134.

[9] T. Irie, G. Yamada, K. Takagi, Natural frequencies of thick annular plates, *Journal of Applied Mechanics* 49 (1982) 633–638.

[10] J. So, A.W. Leissa, Three-dimensional vibrations of thick circular and annular plates, *Journal of Sound and Vibration* 209 (1998) 15–41.

[11] K.M. Liew, B. Yang, Elasticity solutions for free vibrations of annular plates from three-dimensional analysis, *International Journal of Solids and Structures* 37 (2000) 7689–7702.

[12] C.F. Liu, Y.T. Lee, Finite element analysis of three-dimensional vibrations of thick circular and annular plates, *Journal of Sound and Vibration* 233 (2000) 63–80.

[13] D. Zhou, F.T.K. Au, Y.K. Cheung, S.H. Lo, Three-dimensional vibration analysis of circular and annular plates via the Chebyshev–Ritz method, *International Journal of Solids and Structures* 40 (2003) 3089–3105.

[14] W.H. Duan, S.T. Quek, Q. Wang, Free vibration analysis of piezoelectric coupled thin and thick annular plate, *Journal of Sound and Vibration* 281 (2005) 119–139.

[15] P.A.A. Laura, V. Sonzogni, E. Romanelli, Effect of Poisson's ratio on the fundamental frequency of transverse vibration and buckling load of circular plates with variable profile, *Applied Acoustics* 47 (1996) 263–273.

[16] B. Singh, V. Saxena, Axisymmetric vibration of a circular plate with double linear variable thickness, *Journal of Sound and Vibration* 179 (1995) 879–897.

[17] B. Singh, V. Saxena, Axisymmetric vibration of a circular plate with exponential thickness variation, *Journal of Sound and Vibration* 192 (1996) 35–42.

[18] B. Singh, V. Saxena, Transverse vibration of a circular plate with unidirectional quadratic thickness variation, *International Journal of Mechanical Sciences* 38 (1996) 423–430.

[19] A. Shahab, Finite element analysis for the vibration of variable thickness discs, *Journal of Sound and Vibration* 162 (1993) 67–88.

[20] A. Salmane, A.A. Lakis, Natural frequencies of transverse vibrations of non-uniform circular and annular plates, *Journal of Sound and Vibration* 220 (1999) 225–249.

[21] J.H. Kang, A.W. Leissa, Three-dimensional vibrations of thick, linearly tapered, annular plates, *Journal of Sound and Vibration* 217 (1998) 927–944.

[22] J.H. Kang, Three-dimensional vibration analysis of thick, circular and annular plates with nonlinear thickness variation, *Computers and Structures* 81 (2003) 1663–1675.

[23] M. Eisenberger, M. Jabareen, Axisymmetric vibrations of circular and annular plates with variable thickness, *International Journal of Structural Stability and Dynamics* 2 (2001) 195–206.

[24] X. Wang, J. Yang, J. Xiao, On free vibration analysis of circular annular plates with non-uniform thickness by the differential quadrature method, *Journal of Sound and Vibration* 184 (1995) 547–551.

[25] P.A.A. Laura, D.R. Avalos, H.A. Larrondo, V. Sonzogni, Comments on free vibration analysis of circular and annular plates with non-uniform thickness by the differential quadrature method, *Journal of Sound and Vibration* 195 (1996) 338–339.

[26] T.U. Wu, G.R. Liu, Free vibration analysis of circular plates with variable thickness by the generalized differential quadrature rule, *International Journal of Solids and Structures* 38 (2001) 7967–7980.
[27] W.H. Duan, S.T. Quek, Q. Wang, Generalized hypergeometric function solutions for transverse vibration of a class of non-uniform annular plates, *Journal of Sound and Vibration* 287 (2005) 785–807.
[28] M. Koizumi, FGM activities in Japan, *Composites Part B* 28B (1997) 1–4.
[29] J.N. Reddy, C.M. Wang, S. Kitipornchai, Axisymmetric bending of functionally graded circular and annular plates, *European Journal of Mechanics A/Solids* 18 (1999) 185–199.
[30] M. Eisenberger, An exact element method, *International Journal for Numerical Methods in Engineering* 30 (1990) 363–370.
[31] A.W. Leissa, *Vibration of shells*, NASA SP-288, USA, 1973 (reprinted by The Acoustical Society of America, 1993).